



Biosynthesis, Characterization, Adsorption and Antimicrobial Studies of Zirconium Oxide Nanoparticles Using Punica Granatum Extract

Angham Tariq Ali *✉

Department of Chemistry, College of Education
for Pure Sciences, Ibn Al-Haitham
University of Baghdad, Iraq

Lekaa K. Abdul Karem✉

Department of Chemistry, College of Education
for Pure Sciences, Ibn Al-Haitham
University of Baghdad, Iraq

Ewies F. Ewies✉

Organometallic and Organometalloid Chemistry
Departments, Chemical Industries Research Institute,
National Research Centre, ElBohouth St Dokki Cairo,
Egypt P.O 12622.

*Corresponding Author: likaa.k.a@ihcoedu.uobaghdad.edu.iq

Article history: Received 30 December 2022, Accepted 7 February 2023, Published in October 2023.

doi.org/10.30526/36.4.3167

Abstract

In this study we using zirconium sulfate, Punica granatum plant extract, and an alkaline medium, to created ZrO₂ nanoparticles. They were then characterized using a variety of techniques, including FT-IR, UV-visible, atomic force microscopy, X-ray diffraction, transmission electron microscopy, scanning electron microscopy, and energy-dispersive X-ray spectroscopy. The Debye-Scherrer equation was used to calculate the crystal size in X-ray diffraction and found to be 27.82 nm. The particle size of ZrO₂ nanoparticles was determined using atomic force microscopy, scanning electron microscopes, and transmission electron microscopy. Utilizing ZrO₂ NPs, the metal ions M (II) = Co, Ni, and Cu were successfully adsorbed, proving that the three metal ions could be removed from the water at the same time. Over the time frame and under the circumstances, Ni(II) has the highest rate of adsorption. Co, Ni, and Cu ions had removal efficiencies of 32.79%, 75.00%, and 30.20%, respectively. Three concentrations of the ZrO₂ nanoparticles were tested against two types of bacteria, Escherichia coli and staphylococcus, and one type of fungus, Candida, in various concentrations of (25, 50, and 75) mg/L. The outcomes were contrasted with those attained using the medications Amoxicillin and Metronidazole.

Keywords: Adsorption, Antimicrobial, Biosynthesis, Zirconium oxide, X-ray spectroscopy



1. Introduction

The study of nanotechnology involves creating nanoparticles and controlling their physical and chemical properties to maximize their application in a variety of fields for the benefit of people. When compared to bulk materials, changes in certain characteristics, such as size, morphology, and surface area, enhance the biological activity of nanoparticles. In most cases, physical and chemical processes are used to create the nanoparticles. The physical method of synthesis was expensive, and the chemical method uses risky chemicals that have an adverse impact on both people and the environment [1]. So, using microorganisms and plants, scientists developed a method for making nanoparticles that is environmentally friendly and green. The benefit of using plants is that, unlike microbial cultures, they do not need media preparation. The presence of capping, stabilizing, reducing, and oxidizing agents in plant parts, which support their synthesis process, is another benefit [2]. Fruits and plants are abundant in antioxidants, and they also contain a variety of healthy nutrients and small molecules that are good for human health. *Punica granatum* was a type of fruit that was widely consumed in every country (Pomegranate) [3]. Pomegranate peel extract is rich in vitamins, minerals, flavonoids, phenolic acids, and antioxidants [4]. The antimicrobial activity of various pomegranate plant extracts against human pathogens has been demonstrated to be moderate [5]. Numerous studies have documented the use of zirconium oxide (ZrO_2) in a variety of applications, including adsorption, photo-degradation, antimicrobial agents, and structural reinforcement [6]. Enhanced mechanical, thermal, catalytic, and mechanical properties are found in the transition metal zirconium, which also has a high degree of corrosion resistance [7]. Several techniques were used to analyze the obtained ZrNPs' antioxidant potential [8].

2. Materials and Methods

Hydrated zirconium sulfate samples were used and collected *Punica granatum* from a nearby source. ethanol from Sigma Aldrich, NaOH from Alpha India's Alpha Chemical, and $ZrSO_4 \cdot H_2O$ water was all purchased from England, as well as nickel, copper, and cobalt sulfate. A magnetic stirrer, a sensitive electronic balance model as 220C1, a centrifuge type PLC, an electric oven type (FAITHFUL) model -WHL, and 25 AB were among the spectroscopic and microscopic techniques used to create and identify the compounds. FT-IR (8500S) type spectroscopy in the $400\text{--}4000\text{ cm}^{-1}$ range, XRD diffraction type PW1730 (Phillips/ Holland) Shaking Water Bath type (SCL FINETEDI), PH-type UV-visible tape measure (160/Uv) Shimadzu, and (centre of examinations). Use of an X-ray energy dispersion device, SEM type FESEM-EDS Model MIRAI, manufacturer TESCAN, and the Czech Republic of manufacture (EDX). Atomic force microscopes AFM and TEM have the model number EM10C-100Kv.

2.1. Preparation of *Punica Granatum* extract and ZrO_2 NPs

Pomegranate fruits needed for the study were bought at the neighborhood market. Fruits and glassware were cleaned in a hot air oven after being washed in deionized water. The pomegranate peels were taken off later, thoroughly cleaned with deionized water, and allowed to air dry. About 20 grams of dried fruit peels were combined with 100 mL of distilled water and boiled for 10 minutes in an Erlenmeyer flask. Whatman filter paper No. 3 was used to filter the heated liquid after that. The solution was filtered and then put in the fridge. The green synthesis method was used to create ZrO_2 NPs from the preparation process. After adding 0.1M slowly (one drop per second) and stirring for 30 minutes, 50 ml of $ZrSO_4 \cdot H_2O$ and 100 ml of pomegranate peel extract were used. The pH increased to 10–12 after the addition of 50 ml of 1 N NaOH to the solution. The outcome was a precipitate of dark black crystals that were washed with deionized water (all

steps done with a centrifuge, then decantation). It was then baked for four hours at 120°C and sintered for four hours at 250°C. A white powder containing zirconium oxide nanoparticles was created.

2.2. Adsorption study

CoCl₂.6H₂O (10g) was dissolved in 1 litre of distilled water to produce 10000 ppm to make a stock solution. Since 5g of NiCl₂.4H₂O and CuCl₂.2H₂O were dissolved in 1 liter of distilled water to create the stock, its concentration was 5000 ppm. By mixing 0.1 g of the adsorbent nanoparticle with 50 ml of a 1000 ppm liquid solution in a shaker water bath set at 26° C and shaking at 150 rpm, it was possible to adsorb metal ions onto the surface of ZrO₂ NPs. Centrifuging was then used to periodically separate the adsorbent from the solution. Using the calibration curve, the remaining concentration after adsorption was estimated by measuring the clear solution using a visible spectrophotometer [9].

2.3. Biological Activity

Using the disc diffusion method in a nutrient medium (jellos medium) of the Muller Hinton agar type, the antimicrobial activity of the synthetic ZrO₂ NPs at concentrations of approximately (25, 50, and 75) mg/L was checked against two reference bacterial strains, (G+) *S. aureus* and (G-), *Escherichia coli*, as well as the fungus *Candida albicans*. The same process was used to assess the nutrient medium with a potato dextrose base's antifungal activity (agar)[9,10].

3. Result and discussion

3.1. FT_IR spectrum analysis

The Zr-O bond is present in the ZrO₂ structure, as shown by the bands at (435.92-500) cm⁻¹ in the ZrO₂ FTIR spectrum shown in **Figure1**. Other bands may be due to remnants of active groups in the plant extract [11, 12].

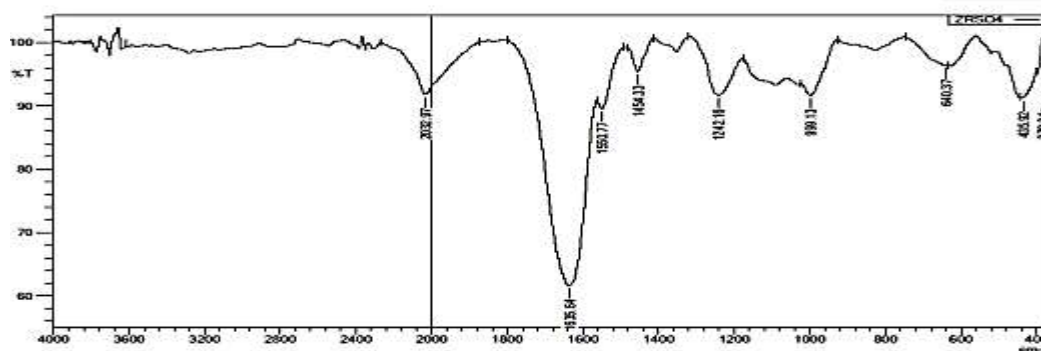


Figure 1: FT-IR spectrum of ZrO₂NPs

3.2. The UV-Visible spectrum

Figure 2 depicts the biosynthesis of ZrO₂NPs' UV-Vis absorption spectrum. The transition hole process between Zr and O caused the absorption peak in this spectrum to appear at 342.0 nm [13].

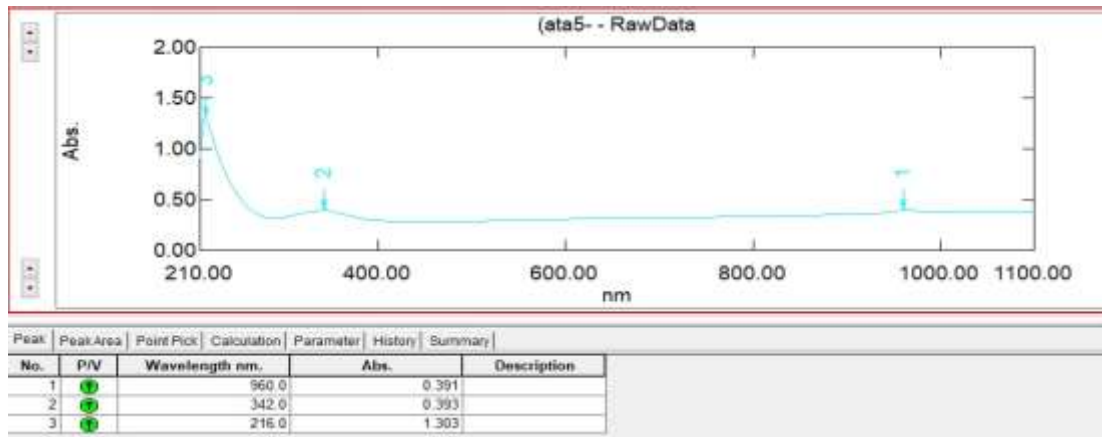


Figure 2. UV-Visible spectrum of ZrO₂Nps

3.3. X-Ray Diffraction (XRD)

According to XRD analysis, orthorhombic ZrO₂ consistent miller indices hkl values (111), (002), (022), (031), (131) crystal planes are allocated to a series of diffraction peaks at 2θ of 15.8451, 18.9344, 24.6488, 25.2519, 26.6040, 34.0037, 39.1056, 46.1781, 51.6897, and 74.4164, respectively. The average crystal size was calculated using the Debye Scherrer equation ($D = 0.9 \lambda / \beta \cos \theta$) where D= the average crystalline size and the Cu K X-ray radiation ($\lambda = 1.5418\text{Å}$), and it was discovered to be 27.82 nm in **Figure 3 and Table 1**.

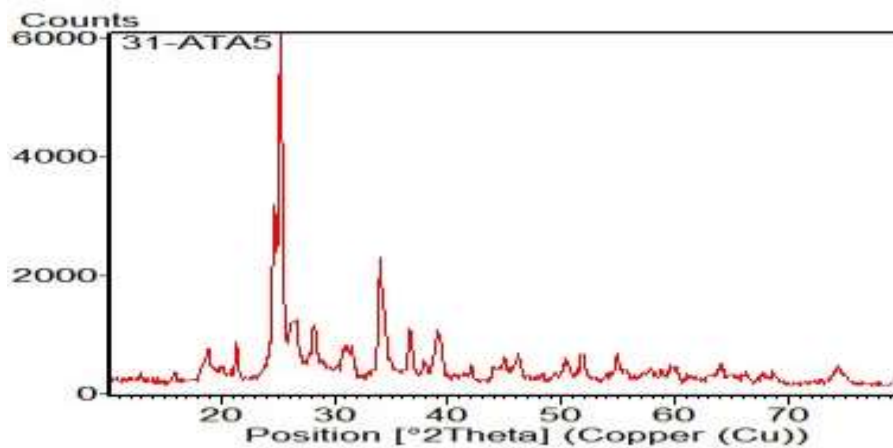


Figure 3. XRD of ZrO₂ NPs

Table 1. The data of XRD for ZrO₂ Nps

Pos. [°2Th.]	Height [cts]	FWHM [°2Th.]	Particle size (nm)	Average crystal size (nm)
15.8451	188.47	0.2952	28.31	
18.9344	614.50	0.2460	34.19	
24.6488	3039.56	0.2460	34.85	
25.2519	5963.14	0.2952	29.71	27.82
26.6040	1061.55	0.2952	30.14	
34.0037	2155.46	0.3444	25.92	
39.1056	825.46	0.5904	15.52	
46.1781	512.50	0.3936	23.99	
51.6897	500.78	0.3444	27.79	
74.4164	294.31	0.8400	12.29	

3.4. EDX

Zirconium and oxygen exhibit the anticipated peaks in the ZrO_2 Nps EDX spectrum. **Figure 4** having a 1:1 ratio between them. The outcomes show how incredibly pure the produced nanoparticles are; real-world estimates from the EDX measurement and basic theoretical calculations also yield similar results [12].

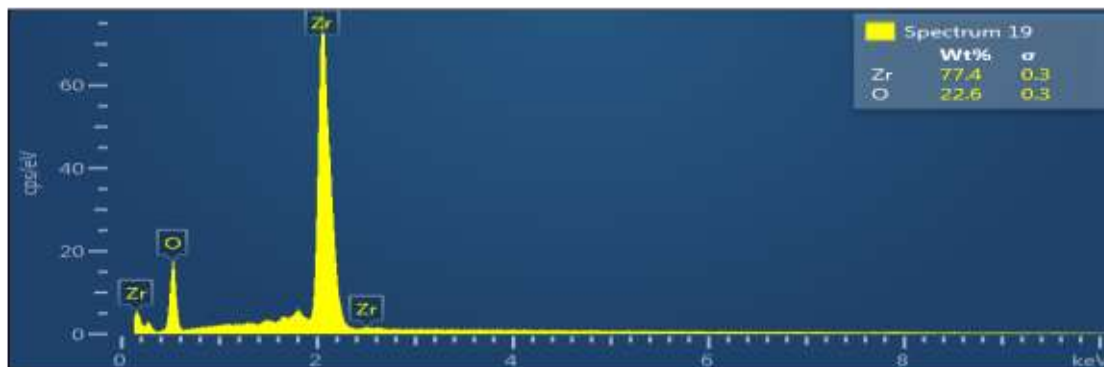


Figure 4. The EDX of ZrO_2 NPs

3.5. SEM and TEM analysis

The morphology and shapes of nanomaterial's were determined using SEM and TEM. SEM and TEM measurements of Figures 5 and 6 show low amounts of rods in nano-structured, unconsolidated shapes of ZrO_2 NPs. The ZrO_2 nanoparticles in the TEM image appeared as a nanoscale UN-consolidated structure. It should be noted that the samples have a high pore content, which makes them stand out in adsorption applications [13]. The TEM image revealed that ZrO_2 nanoparticles were tightly packed. The sample appears to contain measurements of its spherical structural properties that are zero-dimensional (all of the dimensions are nanoscale), which is highly preferred in chemical nature for nanomaterials, though the shape of the sample cannot be determined with absolute certainty due to measurement accuracy [14].

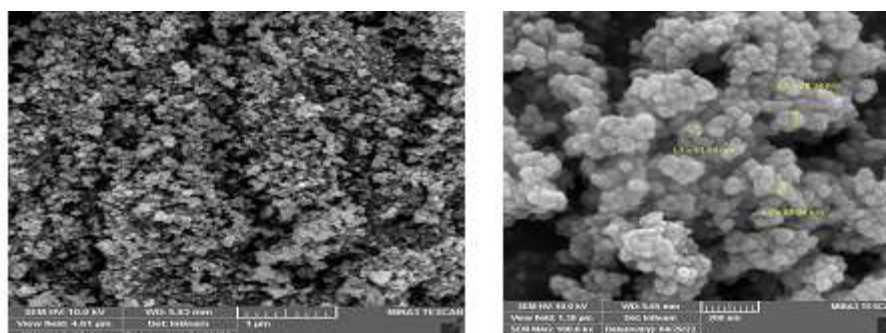


Figure 5. SEM of ZrO_2 NPs.

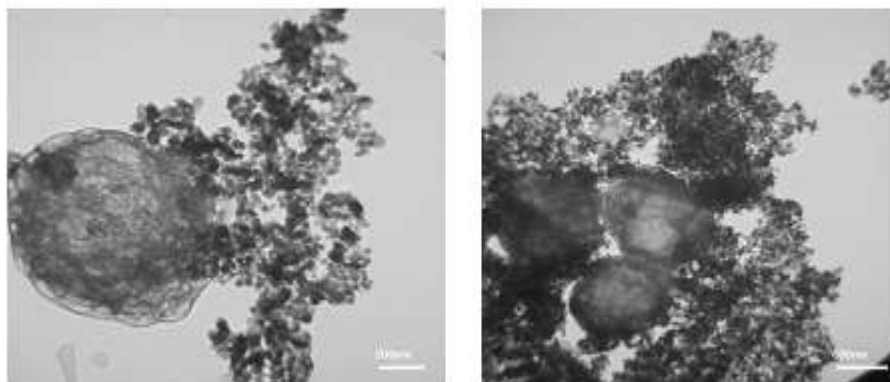


Figure 6: TEM of ZrO₂ NPs

3.6. AFM analysis

AFM surface analysis must be carefully scrutinized because a variety of variables, including the presence of deformations or the existence of image artifacts brought on by a tip and/or contamination, may result in false positives. One of the important factors is whether or not to operate in contact. The degree of surface contact between the sample and its tip, or contact mode, severely degrades ZrO₂ Nps nanoparticles. The tip is placed very close to the sample but not in contact with it; hence, the only mode necessary for this task is the non-contact one. In terms of optical behaviour, **Figure 7** shows the development of three-dimensional spherical clusters of ZrO₂ Nps following metallization [15]. Due to the environmentally friendly synthesis of the nanomaterials, the surface of the sample has pores, is highly rough, and tends to have an amorphous shape. According to the Height Accumulation Distribution Report of ZrO₂ NPs, the prepared oxide nanoparticles have a size range of 17 to 17 nm. This proves that the nano oxide manganese made with pomegranate peel extract actually exists [16,17].

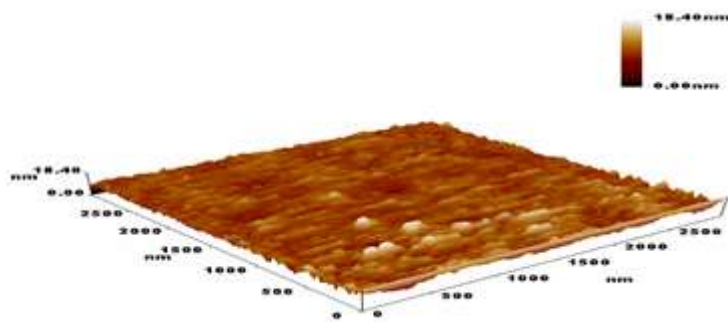
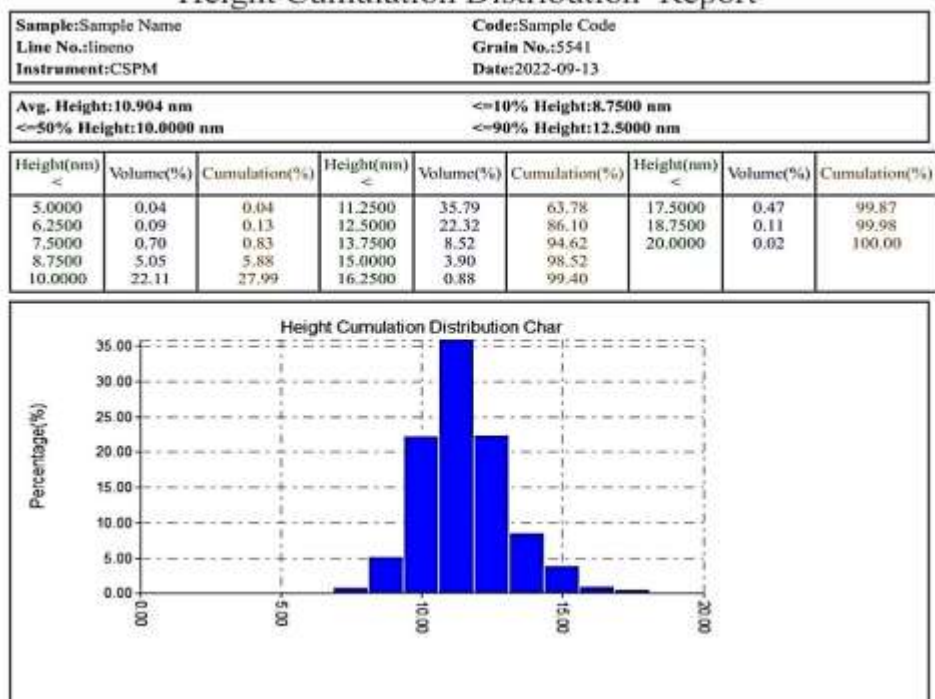


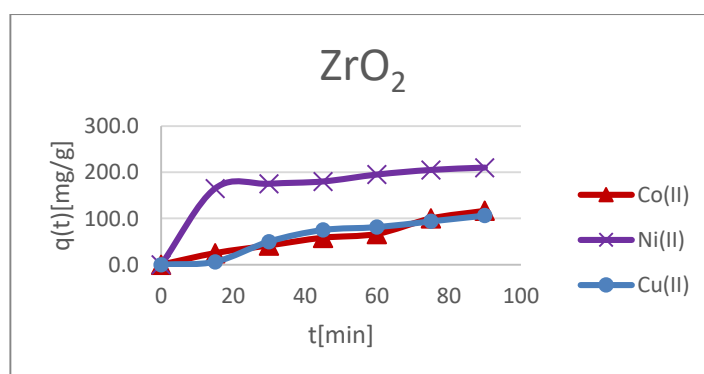
Figure 7. The AFM of ZrO₂ NPs.

Height Cumulation Distribution Report

Figure 8: Height Cumulation Distribution Report of ZrO_2 Nps

3.7. Adsorption Study

In a comparison of the adsorption behaviour of the prepared ZrO_2 nanoparticles, the adsorption time profile for each ion was displayed. The continuous adsorption growth of Co (II) indicates that the process is out of equilibrium and that this is not a simple type of adsorption. Instead, the cobalt chloride salt crystallizes as a result of a precipitation process in which metal oxide nanoparticles serve as crystallization nuclei. Ni (II) and Cu (II) have more pronounced equilibrium plateaus, especially Ni (II) **Figure 9**. The largest surface in an alternative form is ZrO_2 . This arrangement might be the result of convergences in the atomic radius of the V element and the adsorbate metal ions, which make it simple for them to combine with the metal oxide's lattice active sites [18- 20].

Figure 9. Adsorption time evolution of the metal ions on the ZrO_2 surfaces.

According to the time scale and conditions of our experiment, the adsorption rate of Ni(II) is unquestionably the highest on all surfaces, whereas Co(II) and Cu(II) ions are close in magnitude, as shown by the above figures. Charge, size, and electronic interactions all have an impact on the

rate of adsorption [20,21]. The first factor (charge) cannot be the primary cause of this difference because all ions have the same charge. Both the majority of the solution and the adsorbent mass are affected by size during the diffusion process [22-26]. This theory predicts that Co (II), Ni (II), and Cu should have the highest adsorption rates (II), but the rate of decrease in the Co (II) adsorption rate and also the unrestricted linear growth of an adsorbed component indicate that there is still another process taking place in addition to adsorption, and that is the Co (II) oxidation by metal oxide.

3.8. Study of Antimicrobial

Using the agar-well diffusion method[27-29], the antibacterial activity of the synthetic ZrO₂ nanoparticles was examined against the bacteria *Escherichia coli*, *Staphylococcus*, and *Candida* in various concentrations of (25, 50, and 75) mg/L [30]. Amoxicillin and metronidazole were used as drug controls, and DMSO solvent medium served as the antibiotics' controls. By analyzing the zone of growth inhibition against the employed pathogens and varying the concentration of the nanoparticles, the antimicrobial activities of the ZrO₂ nanostructures were assessed. The growth zone inhibition in (mm) of ZrO₂ NPs against the bacterial pathogens two bacteria and one fungus is shown in **Table 2**, **Figure 10** and, **Figure11**.

Table2. The Zone Inhibition in (mm) of ZrO₂NPs against Different Microbial

Conc. mg/L	<i>Escherichia coli</i>	<i>Staphylococcus aureus</i>	<i>Candida albicans</i>
25	4	5	4
50	5	6	5
75	15	13	31

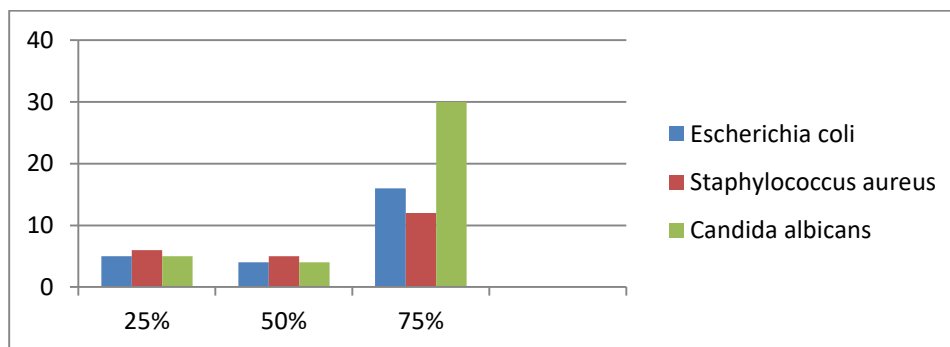


Figure 10. The Antibacterial activity of ZrO₂ NPs.

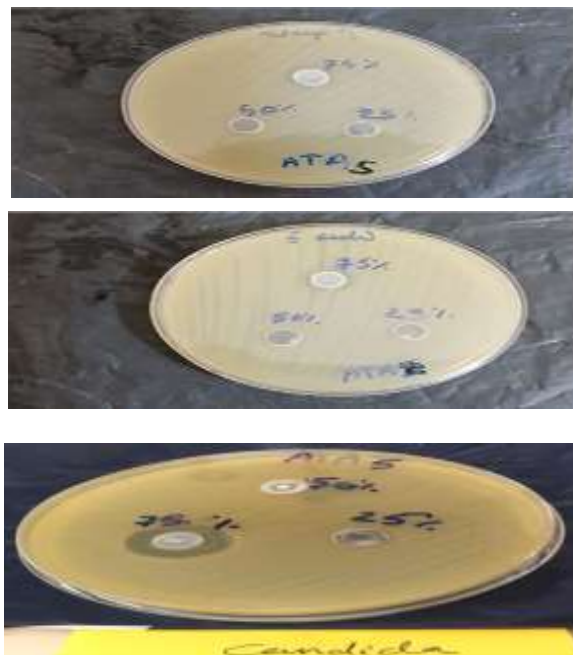


Figure 11. The zone inhibition of growth.

4. Conclusion

Orthorhombic zirconium oxide NPs with a crystal size of 27.82 nm were produced as a result of the presence of $ZrSO_4$. To create ZrO_2 NPs were used as the first ingredient. Manganese oxide exhibited thin sheet cluster morphology in its aggregate form. Because of their antimicrobial activity, *Candida albicans* and *S. aureus* grow noticeably more slowly. Three additional metal ions M(II), Co, Ni, and Cu were also removed from the water by ZrO_2 , in addition to the three other metal ions.

Acknowledgment

The author would like to extend their heartfelt appreciation to the Chemistry Department, College of Education for Pure Sciences at Ibn-Al Haitham University in Baghdad, Iraq, for their generous provision of resources in support of this research endeavor.

Conflict of Interest

The authors declare that they do not have any competing interests.

Funding

The absence of a financial source is evident.

Ethical Clearance

The studies have been approved by the Committee of the (**University of Baghdad College of Education for Pure Sciences, Ibn Al-Haitham**), and have been done by the ethical standards set out in 1964. I confirm that the participant was given a chance to ask questions about the study and that I answered all of their questions correctly and to the best of my ability. I swear that the person's consent was not forced on them and was given freely and voluntarily.

References

1. Rajagopal, G.; Nivetha, A.; Ilango, S.; Muthudevi, G.P.; Prabha, I.; Arthimanju, R. Phytofabrication of Selenium Nanoparticles Using *Azolla Pinnata*: Evaluation of Catalytic Properties in Oxidation, Antioxidant and Antimicrobial Activities, *Journal of Environmental Chemical Engineering* **2021**, *9*, 105483. <https://doi.org/10.1016/j.jece.2021.105483>.
2. Fathima, J.B.; Pugazhendhi, A.; Venis, R. Synthesis and Characterization of ZrO₂ Nanoparticles-Antimicrobial Activity and Their Prospective Role in Dental Care, *Microbial pathogenesis* **2017**, *1*, 245-51. <https://doi.org/10.1016/j.micpath.2017.06.039>.
3. da Silva, A.F.; Fagundes, A.P.; Macuvele, D.L.; de Carvalho, E.F.; Durazzo, M.; Padoin, N.; Soares, C.; Riella, H.G. Green Synthesis of zirconia Nanoparticles Based on *Euclea Natalensis* Plant Extract: Optimization of Reaction Conditions and Evaluation of Adsorptive Properties. *Colloids and Surfaces A: Physicochemical and Engineering Aspects* **2019**, *20*, 123915. <https://doi.org/10.1016/j.colsurfa.2019.123915>.
4. Al-Zaqri, N.; Muthuvel, A.; Jothibas, M.; Alsahme, A.; Alharthi, F.A.; Mohana, V. Biosynthesis of Zirconium Oxide Nanoparticles Using *Wrightia Tinctoria* Leaf Extract: Characterization, Photocatalytic Degradation and Antibacterial Activities. *Inorganic Chemistry Communications* **2021**, *1*, 108507. <https://doi.org/10.1016/j.inoche.2021.108507>.
5. Kumaresan, M.; Anand, K.V.; Govindaraju, K.; Tamilselvan, S.; Kumar, V.G. Seaweed *Sargassum Wightii* Mediated Preparation of zirconia (ZrO₂) Nanoparticles and Their Antibacterial Activity Against Gram Positive and Gram Negative Bacteria. *Microbial pathogenesis* **2018**, *1*, 311-5. <https://doi.org/10.1016/j.micpath.2018.08.060>
6. Karunakaran, G.; Suriyaprabha, R.; Manivasakan, P.; Yuvakkumar, R.; Rajendran, V.; Kannan, N. Screening of in Vitro Cytotoxicity, Antioxidant Potential and Bioactivity of Nano-and Micro-ZrO₂ and-TiO₂ Particles. *Ecotoxicology and environmental safety* **2013**, *1*, 191-7. <https://doi.org/10.1016/j.ecoenv.2013.04.004>.
7. Alsharari S.S.; Alenezi M.A.; Al Tami M.S.; Soliman M. Recent Advances in the Biosynthesis of Zirconium Oxide Nanoparticles and Their Biological Applications. *Baghdad Science Journal* **2022**, 41-57. <https://doi.org/10.21123/bsj.2022.7055>.
8. Salavati-Niasari M. ; Dadkhah M.; Davar F. Pure Cubic ZrO₂ nanoparticles by Thermolysis of a New Precursor. *Polyhedron* **2009**, *28*, 3005-9.
9. Singh A.K.; Nakate U.T. Microwave Synthesis, Characterization, and Photoluminescence Properties of Nanocrystalline Zirconia. *The Scientific World Journal* **2014**, *1*. <https://doi.org/10.1155/2014/349457>
10. Shinde H. M; Bhosale T. T; Gavade N. L; Babar S. B; Kamble R. J; Shirke B. S; Garadkar K. M. Biosynthesis of ZrO₂ Nanoparticles from *Ficus Benghalensis* Leaf Extract for Photocatalytic Activity. *Journal of Materials Science: Materials in Electronics* **2018**, *29*,14055-14064. [10.1007/s10854-018-9537-7](https://doi.org/10.1007/s10854-018-9537-7)
11. Salem, S. S.; Fouda, A. Green Synthesis of Metallic Nanoparticles and Their Prospective Biotechnological Applications: An Overview. *Biological Trace Element Research* **2021**, *199*, 344-370. [10.1007/s12011-020-02138-3](https://doi.org/10.1007/s12011-020-02138-3).
12. Sigwadi R.; Dhlamini M. S.; Mokrani T.; Nonjola, P. Effect of Synthesis Temperature on Particles Size and Morphology of Zirconium Oxide Nanoparticle. In: *Journal of Nano Research*. Trans Tech Publications Ltd **2017**, 18-31. <https://www.scientific.net/JNanoR.50.18>
13. Raghad, D.H; Abdul Jalil; Maryam M.H.M. Jawad; Ahmed N. Abd. Plants extracts as green synthesis of zirconium oxide nanoparticles. *Journal of Gene c and Environmental Resources Conservaon* **2017**, *5*,6-23. https://www.academia.edu/34736142/Plants_extract_as_green_synthesis_of_zirconium_oxide_nanoparticles

14. Karem, L. K. A.; Ali, A. T. Biosynthesis, Characterization, Adsorption and Antimicrobial studies of Manganese oxide Nanoparticles Using Punica Granatum Extract. *Baghdad Science Journal* **2023**, <https://doi.org/10.21123/bsj.2023.8183>.
15. Akhtar K.; Baig J. A.; Kazi T. G.; Afridi H. I.; Talpur F. N.; Solangi I. B.; Samaijo S. Novel fluoride selective voltammetric sensing method by amino phenylboronic acid-zirconium oxide nanoparticles modified gold electrode. *Microchemical Journal* **2022**, 174, 107073. <https://doi.org/10.1016/j.microc.2021.107073>.
16. Rheima AM; Anber AA; Abdullah HI; Ismail AH. Synthesis of alpha-gamma aluminum oxide nanocomposite via Electrochemical Method for Antibacterial Activity. *Nano biomed engineering* **2021**, 13, 1-5.
17. Reczek L.; Michel M.M.; Trach Y.; Siwiec T.; Tytkowska-Owerko M. The Kinetics of Manganese Sorption on Ukrainian Tuff and Basalt-Order and Diffusion Models Analysis. *Minerals* **2020**, 28, 101065. <https://doi.org/10.3390/min10121065>.
18. Karimi F; Ayati A; Tanhaei B; Sanati AL; Afshar S; Kardan A; Dabirifar Z; Karaman C. Removal of Metal Ions Using a New Magnetic Chitosan Nano-bio-adsorbent; A Powerful Approach in Water Treatment. *Environmental Research* **2022**, 203, 111753. <https://doi.org/10.1016/j.envres.2021.111753>.
19. Sadiq Khasro F; Mahmood H.S. Enhancement of Antibacterial Activity of Face Mask with Gold Nanoparticles. *Ibn AL-Haitham Journal For Pure and Applied Sciences* **2022**, 35, 25-31. [10.30526/35.3.2844](https://doi.org/10.30526/35.3.2844).
20. Amer AA; Karem LK. Biological Evaluation and Antioxidant Studies of NiO, PdO and Pt Nanoparticles Synthesized from a New Schiff Base Complexes. *Ibn Al-Haitham Journal For Pure and Applied Sciences* **2022**, 35, 170-182. <https://doi.org/10.30526/35.4.2864>
21. Habib A.A.S. ; Yousif A.M. Effect of Nano-Zirconium Oxide and Other Applications on Cowpea Seedlings Growth Under T Salt Stress. *Iraqi Journal of Science* **2018**, 1006-1011. <https://ijs.uobaghdad.edu.iq/index.php/eijs/article/view/339>
22. Karem, L. K. A.; Ali, A. T. Biosynthesis, Characterization, Adsorption and Antimicrobial Studies of Vanadium Oxide Nanoparticles Using Punica Granatum Extract. *Baghdad Science Journal* **2023**, <https://doi.org/10.21123/bsj.2023.8114>.
23. Abdalsahib, N.M.; Karem L.K.A. Synthesis, Characterization, Antioxidant and Antibacterial Studies for New Schiff Base Complexes Derived from 4-Bromo-O-Toluidine. *International Journal of Drug Delivery Technology* **2023**, 13, 679-685. <http://10.25258/ijddt.13.2.33>.
24. Naji, S.H.; Karim, L.K.A., Mousa, F.H. Synthesis, Spectroscopic and Biological Studies of a New Some Complexes with N-Pyridin-2-Ylmethyl-Benzene-1, 2Diamine. *Ibn AL-Haitham Journal For Pure and Applied Science* **2013**, 26, 193-207. <https://www.iasj.net/iasj/article/72289>.
25. Abdalsahib, N.M.; Karem, L.K.A. Preparation, Characterization, Antioxidant and Antibacterial Studies of New Metal (II) Complexes with Schiff Base for 3-amino-1-phenyl-2- pyrazoline-5-one. *International Journal of Drug Delivery Technology* **2023**, 13, 290-296. <http://10.25258/ijddt.13.2.33>.
26. Baqer, S.R.; Alsammaraie, A.M.A.; Alias, M.; Al-Halbosiy, M.M.; Sadiq, A.S. In Vitro Cytotoxicity Study of Pt Nanoparticles Decorated TiO₂ Nanotube Array. *Baghdad Science Journal* **2020**, 17, 1169-1169. <https://doi.org/10.21123/bsj.2020.17.4.1169>.
27. Mohan, B.; Shaalan, N. Synthesis, Spectroscopic, and Biological Activity Study for New Complexes of Some Metal Ions with Schiff Bases Derived From 2-Hydroxy Naphthaldehyde with 2-amine benzhydrazide. *Ibn AL-Haitham Journal For Pure and Applied Sciences* **2023**, 36, 208-224. <http://doi.org/10.30526/36.1.2978>.
28. Karem, L.K.A.; Radhi, I.M; Mohammed, S.S. Biological Activity of Complexes of Some Amino Acid: Review. *Indian Journal of Forensic Medicine & Toxicology* **2019**, 14, 2254-2261. <https://doi.org/10.37506/ijfmt.v14i4.11888>.

29. Mohammed,S.S.; Karem,L.K.A.; Salman,S.A.; Al-Darwesh, M.Y. Spectroscopic, Thermodynamic and Kinetic Studies of Ligand Complexes Derived From 2-Aminothiophenol. *Biochemical and Cellular Archives* **2020**, *20*, 6435–6439. <https://connectjournals.com/03896.2020.20.6329> .
30. Mohammed, S.S.; Aziz, N. M.; Karem, L.K.A. Preparation and Diagnostics of Schiff Base Complexes and Thermodynamic Study for Adsorption of Cobalt Complex on Iraqi Attapulgitic Clay Surface. *Egyptian Journal of Chemistry* **2021**, *64*, 6913-6920. [10.21608/EJCHEM.2021.75540.3703](https://doi.org/10.21608/EJCHEM.2021.75540.3703).